PNAS

Supplementary Information for

Gas plasma-oxidized sodium chloride acts via hydrogen peroxide in a model of peritoneal carcinomatosis

§Lea Miebach[1,2], §Eric Freund[1,2], Ramona Clemen[1], Stephan Kersting[2], Lars-Ivo Partecke[2,3], *Sander Bekeschus[1]

Dr. Sander Bekeschus
Email: sander.bekeschus@inp-greifswald.de

This PDF file includes:

Materials and Methods

Quantification of reactive oxygen and nitrogen species in the liquids

ROS/RNS quantification in gas plasma-oxidized saline solutions was assessed immediately after gas plasma treatment. Changes in pH were measured using a pH meter (Mettler Toledo, Germany). Relative redox sensors were used to determine short-lived reactive species' presence in oxNaCl solutions. Immediately after gas plasma treatment, aminophenyl fluorescein (APF; indicative of HOCl, $^{\cdot}OH$, $ONOO^-$), hydroxyphenyl fluorescein (HPF; indicative of $^{\cdot}OH$, $ONOO^-$) or diaminophenyl fluorescein (DAF; indicative of $NO^{\cdot}$) were added at a concentration of 5 µM to 100 µl sample respectively. Immediately after, fluorescence was acquired at λ_{ex} = 485 nm and λ_{em} = 535 nm using a multiplate reader (F200; Tecan, Switzerland). As a reference for ROS/RNS delivery in direct (in vitro) gas plasma treatment regimes, probes were added to 1 ml NaCl prior to 60 s gas plasma treatment following fluorescence measurements with similar acquisition setups. All values were background subtracted. Hydrogen peroxide (H_2O_2) deposition was determined using the titanyl sulfate assay. Briefly, gas plasma-oxidized saline solutions were diluted 1:3 in titanyl sulfate, and absorbance was measured at 407 nm using a monochromator-based microplate reader (M200; Tecan, Switzerland). Concentrations of nitrite (NO_2^-) and nitrate (NO_3^-) were determined using the Griess Assay according to the supplier's instructions. Absorbance was measured at 540 nm using a multimode plate reader (M200; Tecan, Switzerland). Hypochlorous acid (HOCl) production was assessed utilizing the taurine chloramine assay. Briefly, 198 µl of oxNaCl solutions were mixed with 2 µl of a taurine buffer. Immediately after, 50 µl developer solution consisting of sodium acetate (270 mM, pH = 5.4), sodium iodide (100 µM), and tetramethylbenzidine in dimethylformamide (2 mM) was added. Absorbance was measured at 645 nm. The atmospheric plasma jet kINPen [1], which was operated with helium-oxygen (He/O_2) as feed gas that was previously shown to generate HOCl in liquids [2], was used as a positive control. Absolute concentrations of reactive species were calculated against a standard curve in all assays.

Cell culture and treatment procedure

The human cancer cell lines HT-29 (colon adenocarcinoma; ATCC: HTB-38), Panc-01 (pancreatic epitheloid carcinoma; ATCC: CRL-1469), and SKOV3 (serous ovarian carcinoma; ATCC: HTB-77) were cultured in Dulbecco's modified Eagles Medium (DMEM; Pan Biotech, Germany) supplemented with 10 % fetal bovine serum, 1 % glutamine, and 1 % penicillin and streptomycin (all Corning, Germany). Non-malignant HaCaT keratinocytes (ATCC: CVCL-0038) were cultured in Roswell Park Memorial Institute (RPMI) 1640 medium (Pan Biotech, Germany) supplemented with 10 % fetal bovine serum, 1 % penicillin and streptomycin, and 1 % glutamine (all Corning, Germany). Cells were kept under standard culture conditions at 37 °C, 95 % humidity, and 5 % CO_2 in a cell culture incubator (CB210; Binder, Germany). Twenty-four hours prior to experiments, cells were seeded at a density of either 1×10^4 (96-well flat-bottom plates) or 1×10^5 (24-well flat-bottom plates; both Eppendorf, Germany) cells per well. The cell culture medium was completely removed on the day of experiments and replaced with 100 µl (96-well plates) or 1 ml (24-well plates) of NaCl, oxNaCl, or cmc. After 2 h exposure, liquids were again replaced with fresh cell culture medium. In some assays as control, the H_2O_2-scavenging enzyme catalase (cat; Sigma-Aldrich, Germany) at a 20 µg/ml concentration was added to 50 ml of 0.9 % NaCl prior to 30 min gas plasma. Catalase-supplemented oxNaCl solutions (+cat) were generated as described in the methods in the main text and stored the same way at -20°C until further experiments were performed.

Intracellular reactive species assessment

Endogenous ROS/RNS formation was assessed 4 h after exposure to NaCl, oxNaCl, or cmc solutions. Cells were stained with 1 µM 2',7'-dichlorodihydrofluorescein diacetate (H_2-DCF-DA) and 1 µM DAPI (4′,6-diamidino-2-phenylindole; BioLegend, The Netherlands) for live-dead discrimination for 30 min at 37 °C. Non-fluorescent H_2-DCF-DA is converted to fluorescent 2',7'-dichlorodihydrofluorescein (DCF) upon cleavage by intracellular esterases and subsequent

oxidation in the presence of reactive species. After washing, DCF fluorescence was determined using high content imaging (Operetta CLS; PerkinElmer, Germany). Images were acquired in brightfield and fluorescence channels (λ_{ex} 475nm and λ_{em} 525nm for DCF; λ_{ex} 365 nm and λ_{em} 465 nm for DAPI) using a 20x air objective (NA = 0.4). Experimental setup and image analysis were performed using Harmony 4.9 analysis software (PerkinElmer, Germany).

Intracellular glutathione levels

Relative intracellular levels of oxidized (GSSG) glutathione were determined to assess the cellular redox capacity 24 h after exposure to oxidized saline solutions. Briefly, cells were stained with a glutathione detection probe (Kerafast, USA) for 1 h following high content imaging (Operetta CLS; PerkinElmer, Germany) at λ_{ex} 475 nm and λ_{em} 610 nm. Images were recorded in digital phase contrast (DPC) and respective fluorescence channels in at least nine fields of view (FoV) per well using a 20x air objective (NA = 0.4). Experimental setup and image analysis were done using Harmony 4.9 software (PerkinElmer, Germany).

Metabolic activity

Metabolic activity was investigated 20 h after exposure to 100 µl of oxidized saline solutions in 96-well plates. Briefly, cells were incubated with 100 µM of 7-hydroxy-3H-phenoxazin-3-on-10-oxid (resazurin; Alfa Aesar, Germany) for 4 h. In living cells, non-fluorescent resazurin is metabolized into fluorescent resorufin in a $NADH/H^+$-dependent reaction [3], thereby indicating the cell's metabolic state. Resorufin fluorescence was determined at λ_{ex} 530 nm and λ_{em} 590 nm using a microplate reader (F200; Tecan, Switzerland).

Viability and immunogenic cell death

Tumor-toxicity of oxidized saline solutions was characterized 24 h after treatment in 24-well plates using flow cytometry. Cells were stained with DAPI, caspase 3/7 detection reagent (ThermoFisher, Germany), and anti-calreticulin (CRT) monoclonal antibodies conjugated to phycoerythrin (PE; ENZO Life Sciences, Germany) for 30 min at 37 °C in the dark. Cells were washed and acquired with a four-laser flow cytometer (CytoFLEX S; Beckman-Coulter, Germany). Gating and quantification of mean fluorescence intensities was performed using Kaluza 2.1.3 analysis software (Beckman-Coulter, Germany).

3D tumor spheroids

For 3D tumor spheroid experiments, 5×10^3 cells in 150 µl cell culture medium per well were seeded in a 96-well ultra-low attachment plate (PerkinElmer, Germany). After centrifugation, cells were incubated for 2 days to allow spheroid formation. Prior to treatment with oxidized saline solutions, 100 µl of cell culture medium was exchanged for 100 µl of respective liquids following staining with 1 µM Sytox Blue (ThermoFisher, Germany). Images in brightfield and fluorescence channels (λ_{ex} = 365 nm and λ_{em} = 465 nm for Sytox Blue detection) were acquired after 0 h, 24 h, 48 h, and 72 h. Harmony 4.9 software (PerkinElmer, Germany) was used for algorithm-based quantitative image analysis.

PBMC isolation and generation of monocyte-derived dendritic cells

Human peripheral blood mononuclear cells (PBMCs) were isolated from healthy donors by density gradient centrifugation using lymphocyte separation medium (VWR, Germany). The blood was obtained from a blood bank and de-identified prior to use in your study. For lysis of residual erythrocytes, red blood cell (RBC) lysis buffer (BioLegend, The Netherlands) was used. Monocytes were isolated via $CD14^+$ microbead (Miltenyi Biotec, Germany) selection according to the manufacturer's protocol and subsequently seeded in 24-well suspension plates (Sarstedt, Germany) in 500 µl RPMI cell culture medium supplemented with 10 % fetal bovine serum, 1 % glutamine, 1 % penicillin and streptavidin (all Pan Biotech) at a density of 1×10^5 cells per well. To

initiate differentiation to monocyte-derived $CD11c^+$ dendritic cells (DC), 800 IU (international units) granulocyte-macrophage colony-stimulating factor (GM-CSF) and 500 IU interleukin (IL) 4 (all PeproTech, Germany) were added. Cells were re-stimulated on day two with equivalent amounts of GM-CSF and IL-4.

DC maturation and phagocytosis assessment

Immature DCs were challenged with oxidized tumor cells at a 1:1 effector-target ratio to investigate the capacity of oxNaCl and cmc. Phagocytosis of tumor cell material by DCs was evaluated after 6 h of co-culture. Discrimination of co-cultured cell populations by flow cytometric analysis (CytoFLEX LX; Beckman-Coulter) was achieved by pre-labeling using Vybrant DiD (tumor cells) and DiO (DCs) cell-labeling solutions (ThermoFisher, Germany). The percentage of DCs with phagocytosed tumor material was determined as $DiD^+/CD11c^+$ cells. Assessment of surface-expressed maturation markers was performed in parallel at 6 h. Briefly, co-cultured cells were harvested and stained with monoclonal antibodies (conjugate) targeting CD11c (PE-Cyanine 7), HLA-DR (Alexa Fluor 700), CD86 (PE), and DAPI (all BioLegend, The Netherlands). Additionally, cells were stained with iFluor 860 maleimide (AAT Bioquest, USA) for live-dead cell discrimination using 808 nm laser excitation.

Quantification of chemokines and cytokines

Chemokine and cytokine analysis in co-culture supernatants was done using a bead-based sandwich multi-analyte assay (LegendPLEX; BioLegend, The Netherlands) according to the manufacturer's instructions. The assay panel contained beads targeted against IL1β, IL2, IL6, IL8, IL10, IL18, interferon (IFN) α2, IFNβ, IFNγ, tumor necrosis factor (TNF) α, transforming growth factor (TGF) β1, C-x-C motif chemokine ligand (CXCL) 10, and CC-chemokine ligand (CCL) 4. Beads were labeled with fluorescent detection antibodies, and samples were acquired using flow cytometry (CytoFLEX S; Beckman-Coulter). Absolute concentrations of respective analytes were calculated against a standard curve using specific data analysis software (Vigene Tech, USA).

RNA isolation and NanoString technology

RNA was isolated from tumor cells 4 h after exposure to oxidized saline solutions using an RNA isolation kit (Bio & Sell, Germany) according to the supplier's protocol. The RNA concentration of each sample was determined using fluorescent RNA labeling (Quant-it RiboGreen RNA Reagent; ThermoFisher, Germany) and a fluorometer (DS-11 FX; DeNovix, Germany). Absolute concentrations were calculated against a standard curve. Subsequent gene expression analysis was performed using the NanoString nCounter technology (NanoString Technologies, USA), which directly evaluates RNA levels without prior complementary DNA (cDNA) synthesis. Briefly, 50 ng RNA per sample was hybridized for 24 h at 65 °C with a customized reporter and capture ProbeSet targeting 90 transcripts. Immediately after, samples were loaded into the nCounter SPRINT cartridge and processed by the NanoString nCounter system. Differential gene expression analysis was performed using the nSolver software. Pathway enrichment analysis was evaluated using Gene Set Enrichment Analysis Software (GSEAS) [4,5] and processed with Cytoscape [6] and R-Studio (version 1.4.1717; USA).

Western blot

Cells were pelleted 6 h after treatment and lysed in RIPA buffer containing protease and phosphatase inhibitors (cOmplete Mini, phoSTOP, PMSF; Sigma-Aldrich). Protein expression levels of spliced XBP-1 (XBP-1s) were assessed using appropriate monoclonal antibodies (BioLegend, The Netherlands) and capillary-based gel electrophoresis performed via the WES system (ProteinSimple, Germany) according to the supplier's instructions. Band intensities were quantified using Compass for Simple Western Software and normalized to housekeeping control GAPDH expression.

Tumor-chorioallantois (TUM-CAM) membrane model (*in ovo*)
In ovo (sometimes referred to as *in vivo* studies in chicken embryo CAMs) studies were performed as previously described [7] to investigate the treatment efficacy of oxidized saline solutions on vascularized, three-dimensional tumor organoids. Briefly, specific pathogen-free eggs (Valo BioMedia, Germany) were incubated in a dedicated breeding incubator (Hemel, Germany) at 37 °C and 60 % humidity for 6 d until the pointed poles were carefully punctured using a cannula (20G, Sterican; Braun, Germany). By that, an air cell was created between the chorioallantois membrane (CAM) and eggshell, allowing to cut out a small window at the punctured side for tumor cell inoculation on day 8. Here, 1×10^6 tumor cells together with 1×10^6 monocyte-derived $CD11c^+$ dendritic cells in 15 µl matrigel (Corning, Germany) were seeded in a silicone ring that was placed on the CAM. Eggs were incubated for another 4 d to allow the growth of solid tumors. For treatment on day 12, 100 µl of oxidized saline solutions were transferred into the silicone ring on top of the fully vascularized tumors. Eggs were sacrificed on day 14, and tumor weight was assessed after careful excision.

Nuclear translocation of activating transcription factor 6
Nuclear translocation of activating transcription factor 6 (ATF6) was determined using high content imaging. Briefly, cells were fixed 4 h after exposure to the respective treatment solutions in 96-well glass-bottom plates using 4 % paraformaldehyde (PFA) following permeabilization with Intracellular Staining Permeabilization Wash Buffer (BioLegend, The Netherlands). Cells were stained with purified anti-ATF6 monoclonal antibodies (BioLegend, The Netherlands) at 4 °C overnight, followed by incubation with AF594 goat anti-Rat IgG secondary antibodies for 2 h at room temperature in the dark. Nuclei were counterstained with DAPI. Images were acquired in brightfield and fluorescence channels (λ_{ex} 560 and λ_{em} 590 nm for ATF6; λ_{ex} 365 nm and λ_{em} 465 nm for DAPI) using a 20x air objective (NA = 0.4). Harmony 4.9 software (PerkinElmer, Germany) was used for algorithm-based quantitative image analysis.

TUNEL staining
Terminal deoxynucleotidyl transferase dUTP nick end labeling (TUNEL) technology (In Situ Cell Detection Kit, Fluorescein; Sigma-Aldrich, Germany) was used to evaluate the extent of apoptosis in peritoneal cancer nodules isolated from tumor-bearing mice after repetitive lavage with oxidized saline solutions. Therefore, ultra-thin tissue sections from cryopreserved tumor nodules were prepared using a cryotome (Cryostat CM1950; Leica, Germany) following tissue staining according to the supplier's instructions and additional counterstaining of nuclei with DAPI. Images of stained tissue sections were acquired in appropriate fluorescence channels (λ_{ex} 365 nm and λ_{em} 465 nm for DAPI; λ_{ex} 475 nm and λ_{em} 525 nm for TUNEL) using a 20x air objective (NA = 0.4) and a high content imaging device (Operetta CLS; PerkinElmer, Germany). Algorithm-based object segmentation and quantification were performed using Harmony 4.9 software (PerkinElmer, Germany).

Dose-dependency of surface and ICD-related marker expression in tumor cells
To evaluate dose-dependent effects on ICD-related marker expression, tumor cells were exposed to increasing concentrations (25, 50, 100, 200 µM) of H_2O_2 in 0.9 % NaCl for 2 h. Immediately after, liquids were exchanged with fresh cell culture media. Marker expression profiles were evaluated after 6 h using flow cytometry. Briefly, cells were detached using accutase and stained using two distinct staining panels consisting of monocloncal antibodies targeted against (conjugate) a) CD47 (PerCp-Cy5.5), TNFRI (FITC), TNFRII (AF594; all BioLegend, The Netherlands), and DAPI, and b) CRT (AF647), HSP70 (PE), HMGB1 (PerCp; all BioLegend, The Netherlands) and iFluor maleimeide 860 (AAT Bioquest, USA). After washing, cells were acquired using flow cytometry (CytoFLEX S and CytoFLEX LX; Beckman-Coulter, Germany). Likewise, experiments were performed using increasing dosages of oxNaCl (10, 30, 60, 120 min). Data were evaluated using Kaluza 2.1.3 analysis software (Beckman-Coulter, Germany).

Cell cycle analysis
Twenty-four hours after exposure to NaCl, cells were detached using accutase followed by fixation and permeabilization using ice-cold ethanol for 1 h at 4 °C. Immediately after, cells were stained with 10 µM DAPI for 30 min at 37 °C. After washing and resuspending in PBS-DAPI, cells were acquired using flow cytometry (CytoFLEX S; Beckman-Coulter, Germany) and evaluated using Kaluza 2.1.3 analysis software (Beckman-Coulter, Germany).

Hen's egg chorioallantoic membrane (HET-CAM) irritation assay
The HET-CAM assay was performed as a benchmark test to assess the tissue tolerability of oxNaCl and cmc. Briefly, fertilized chicken eggs were incubated for seven days until the pointed pole was punctured using a cannula. By that, an air hole was created that was windowed on day eight. Two hundred microliters of NaCl, oxNaCl, or cmc were added to the CAM. As a reference, 2 % H_2O_2, a substance approved as an antiseptic in endodontic treatments in dentistry, was tested in parallel. The H_2O_2 concentration in that solution is about 8000-times higher than the H_2O_2 concentration in oxNaCl and cmc employed in this study. Adverse CAM reactions were monitored by taking photographic images immediately, 5 min, 24 h, and 48 h after treatment. The irritation potential of the respective substances was scored blinded, referring to in-house scoring parameters as in principle described before [8].

Statistical analysis
Data are from at least three independent experiments. Graphing and statistical analysis were performed using Prism 9.3.1 (GraphPad Software, USA) and t-test or one-way or two-way analysis of variances (ANOVA) as indicated in the figure legends. Data show mean ± standard error of the mean (SEM) if not indicated otherwise. Levels of significance were indicated as follows: ns = non-significant, p = 0.05 (*), p = 0.01 (**), p = 0.001 (***).

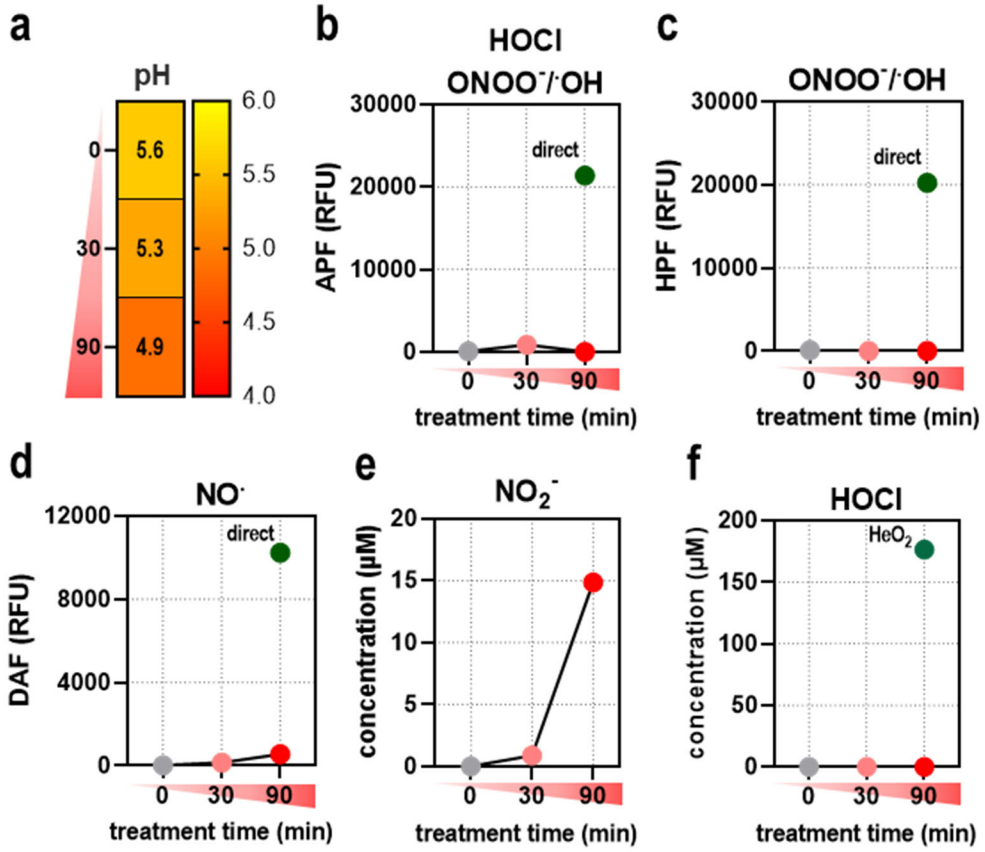

Fig. S1. Quantification of reactive oxygen and nitrogen species in oxNaCl solutions. (**a**) changes in pH in oxNaCl; (**b-d**) relative fluorescence intensities of (**b**) aminophenyl fluorescein (APF; indicative of HOCl, ·OH, $ONOO^-$), (**c**) hydroxyphenyl fluorescein (HPF; indicative of ·OH, $ONOO^-$), and (**d**) diaminophenyl fluorescein (DAF; indicative of NO·) added to oxNaCl after gas plasma treatment, the green dot indicates ROS delivery into NaCl during gas plasma treatment; (**e-f**) quantification of (**e**) nitrite (NO_2^-) and (**f**) hypochlorous acid (HOCl) with the He/O_2 gas plasma regime [9] as a reference for the generation of the latter (green dot). The heat map shows median. Graphs show mean.

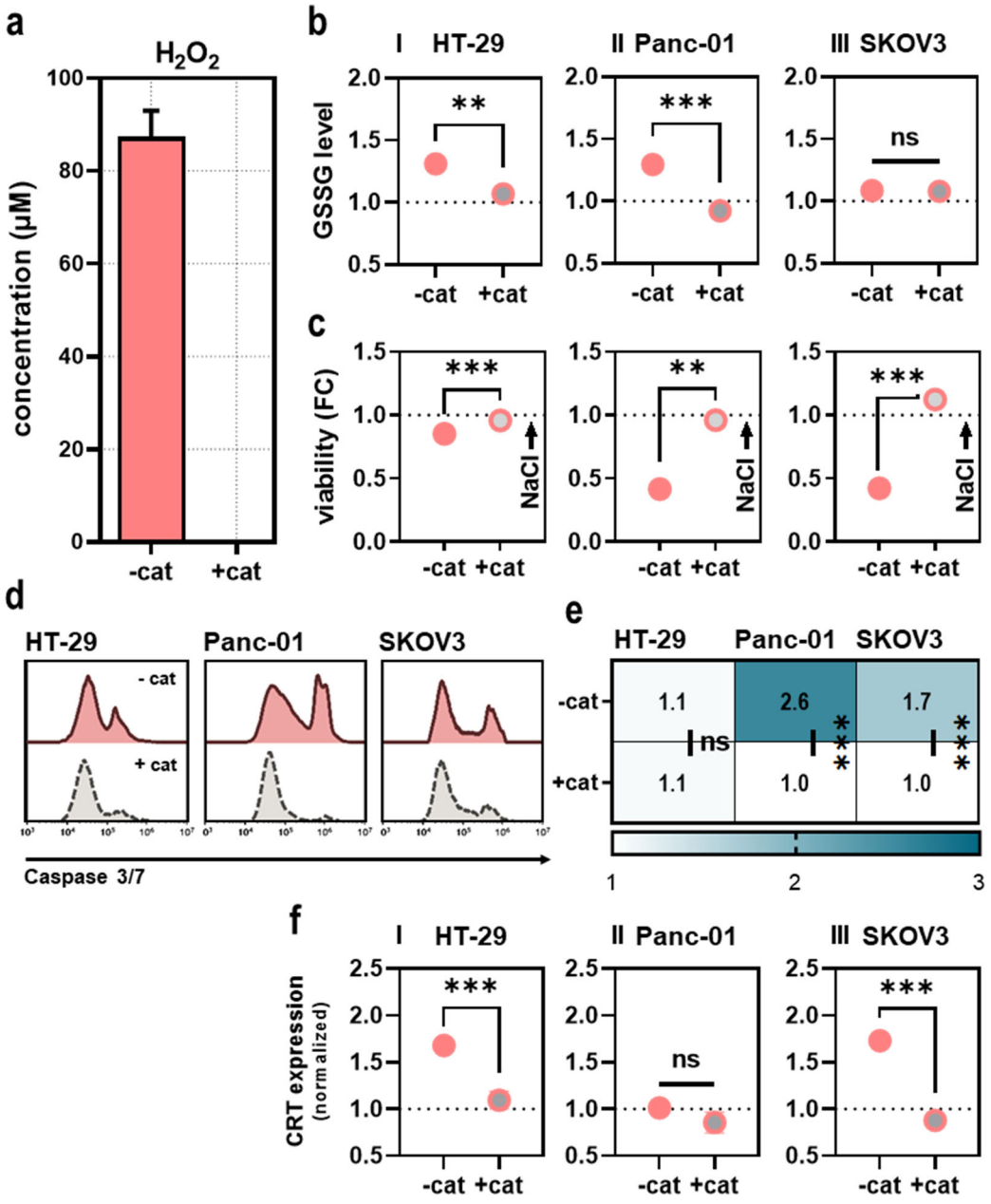

Fig. S2. Catalase attenuates anti-tumor effects of oxNaCl. (**a**) Quantification of H_2O_2 in oxNaCl with or without the addition of catalase (cat) prior to gas plasma treatment; (**b**) quantification of GSSG levels in (**I**) HT-29, (**II**) Panc-01, and (**III**) SKOV3 cells 24 h after exposure to oxNaCl ± cat; (**c**) viability of (**I**) HT-29, (**II**) Panc-01, and (**III**) SKOV3 cells 24 h after exposure to oxNaCl ± cat; (**d-e**) representative flow cytometry intensity histograms of caspase 3/7 activation (**d**) and quantification thereof (**e**); (**f**) ecto-CRT expression of (**I**) HT29, (**II**) Panc-01, and (**III**) SKOV3 cells 24 h after exposure to oxNaCl ± cat. All values were normalized to NaCl-treated controls (dotted line). Bar graphs show mean ± SEM. Dot plots show mean. Statistical analysis was performed using one-way analysis of variance (ANOVA) (**p<0.01, ***p<0.001), ns = non-significant.

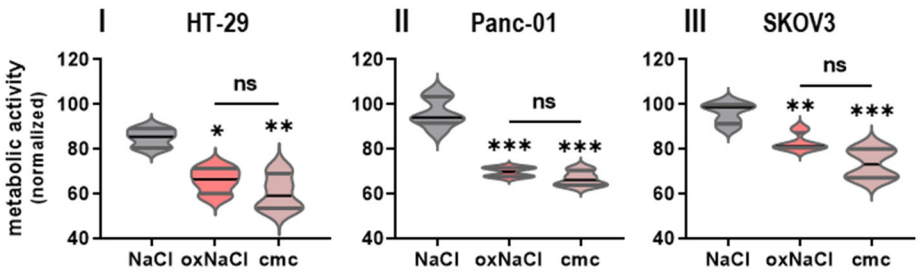

Fig. S3. oxNaCl and cmc solutions equally reduce metabolic activity in human tumor cells. Metabolic activity 24 h after exposure to NaCl, oxNaCl, or cmc solutions in (**I**) HT-29, (**II**) Panc-01, and (III) SKOV3 cells. Violin plots show median ± interquartile range. Statistical analysis was performed using one-way analysis of variance (ANOVA) (*p<0.05, **p<0.01, ***p<0.001), ns = non-significant. oxNaCl = gas plasma-oxidized saline. cmc = concentration-matched control.

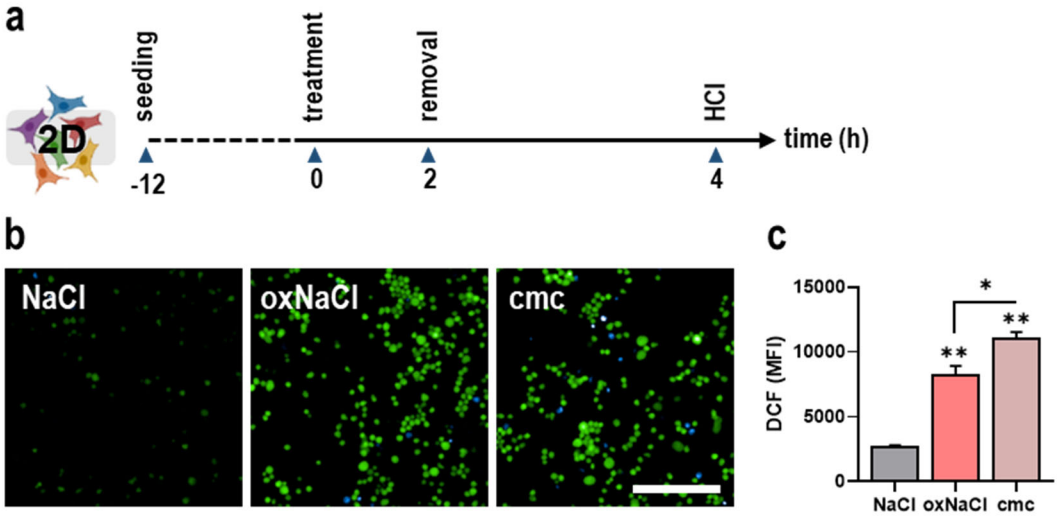

Fig. S4. oxNaCl and cmc solutions equally trigger endogenous ROS amplification. (**a**) schematic overview of experimental procedure; (**b**) representative images of H_2-DCF-DA staining 4 h after exposure to NaCl, oxNaCl, or cmc solutions; (**c**) quantification of DCF fluorescence intensity in viable cells using algorithm-driven high content imaging (HCI). Bar graphs show mean ± SEM. Statistical analysis was performed using one-way analysis of variance (ANOVA) (*p<0.05, **p<0.01), scale bar = 200 µm, ns = non-significant. oxNaCl = gas plasma-oxidized saline. cmc = concentration-matched control.

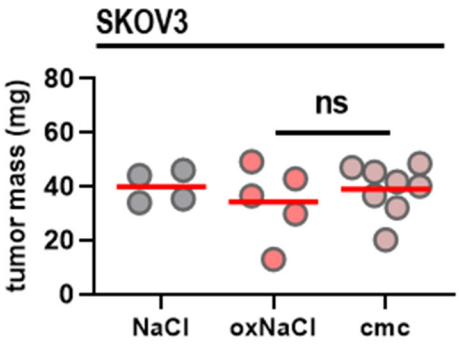

Fig. S5. oxNaCl and cmc solutions do not reduce tumor burden in SKOV3 monoculture tumors grown *in ovo*. Tumor mass of explanted SKOV3 tumors grown *in ovo*. Short black lines indicate the median. Statistical analysis was performed using one-way analysis of variance (ANOVA), ns = non-significant. oxNaCl = gas plasma-oxidized saline. cmc = concentration-matched control.

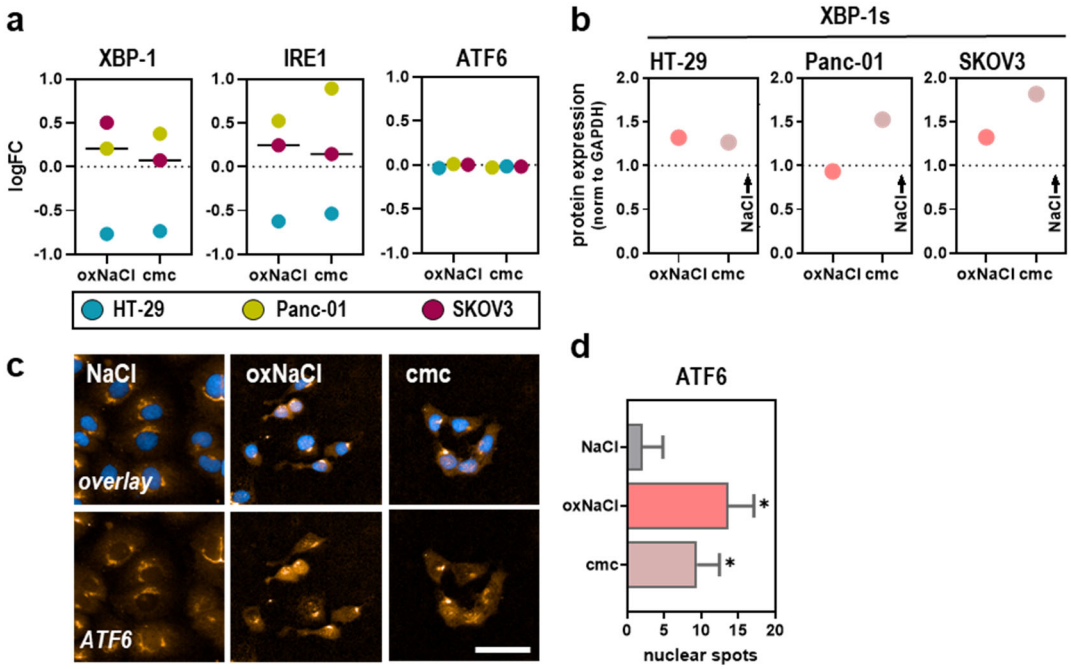

Fig. S6. oxNaCl and cmc solutions equally induce activation of transcription factors involved in the unfolded protein response. (**a**) differential gene expression of XBP-1, IRE1, and ATF6 4 h after exposure to oxNaCl or cmc; (**b**) quantification of XBP-1 band intensities normalized to GAPDH housekeeping control; (**c-d**) representative images of activating transcription factor (ATF) 6 staining (**c**) followed by algorithm-based nuclear spot analysis and quantification thereof (**d**). Bar graphs show mean ± SEM. Statistical analysis was performed using one-way analysis of variance (ANOVA) (*$p<0.05$), scale bar = 100 µm. oxNaCl = gas plasma-oxidized saline. cmc = concentration-matched control.

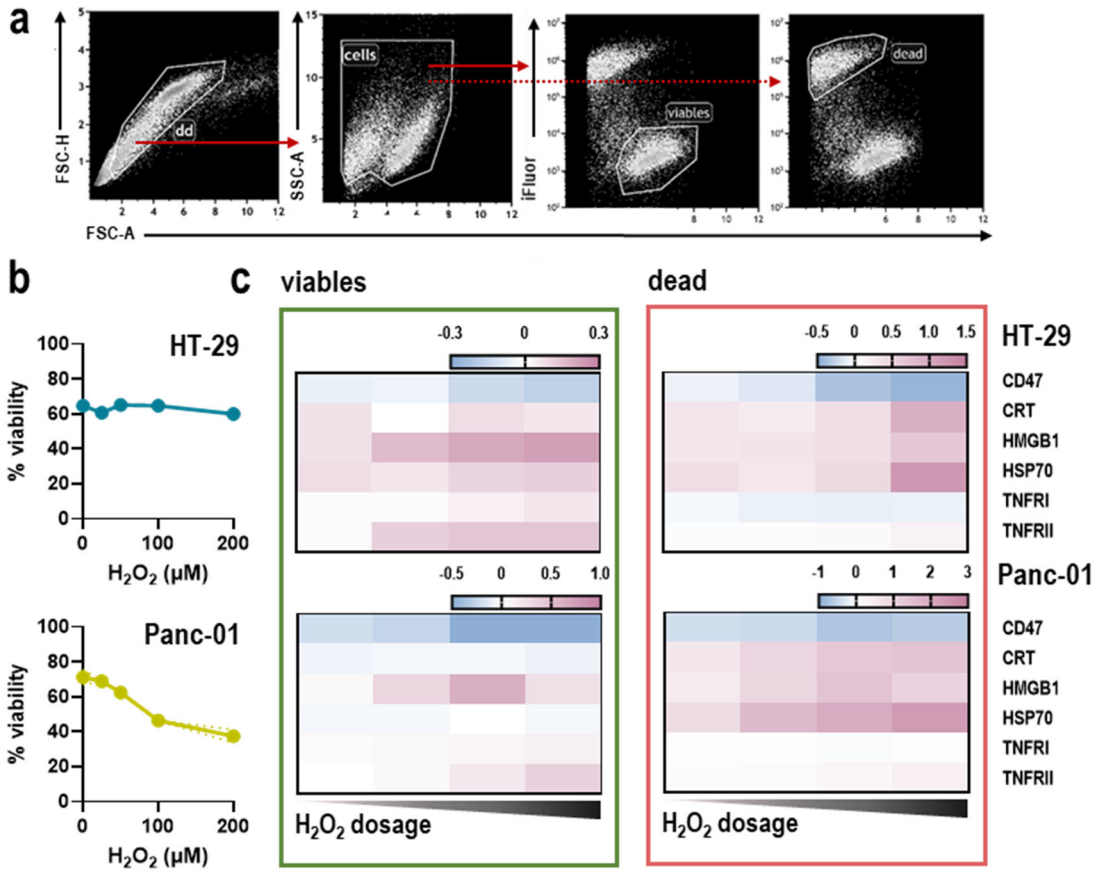

Fig. S7. Comparison of immune and ICD-related marker expression in viable versus dead cells after exposure to increasing dosages of H_2O_2. (**a**) representative flow cytometry dot plots of gating strategies to determine the surface expression of immune-related and ICD markers in viable and dead cells; (**b**) viability of HT-29 and Panc-01 cells 6 h after exposure to increasing dosages of H_2O_2; (**c**) surface expression of CD47, calreticulin (CRT), high mobility group box protein (HMGB) 1, heat shock protein (HSP) 70, and tumor necrosis factor receptor (TNFR) I and II in viable and dead HT-29 and Panc-01 cells normalized to NaCl treated controls. Graphs show mean ± SEM. Heat map shows median.

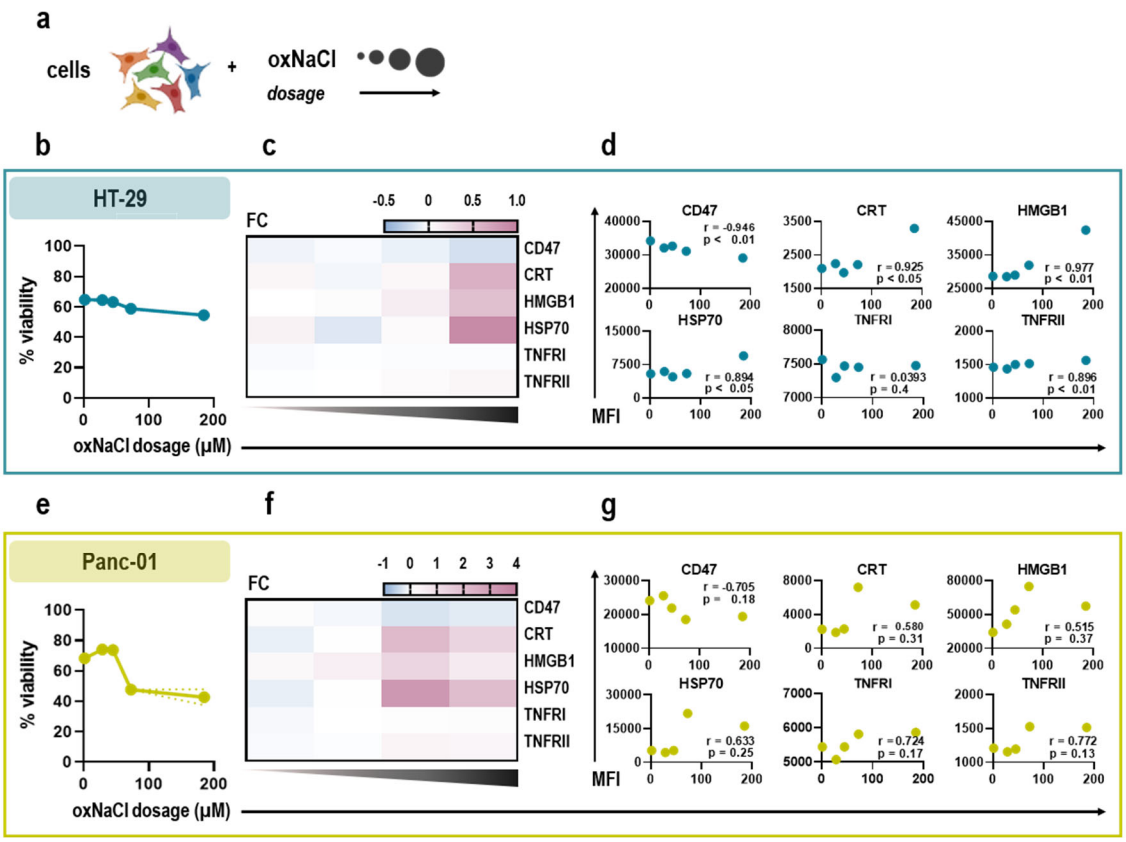

Fig. S8. Immune and ICD-related marker expression after exposure to increasing dosages of oxNaCl solutions. (**a**) schematic overview of the experimental procedure; (**b,e**) viability of HT-29 (**b**) and Panc-01 cells (**e**) 6 h after exposure to increasing dosages of oxNaCl (gas plasma treatment time: 10 min, 30 min, 60 min, 120 min); (**c,f**) surface expression of CD47, CRT, HMGB1, HSP70, TNFRI, and TNFRII in HT29 (**c**) and Panc-01 cells (**f**) normalized to NaCl treated controls; (**d,g**) Pearson's correlation co-efficient of marker expression (mean fluorescence intensities (MFI) against oxNaCl gas plasma treatment time in HT-29 (**d**) and Panc-01 cells (**g**). Graphs show mean ± SEM. Heat map shows median.

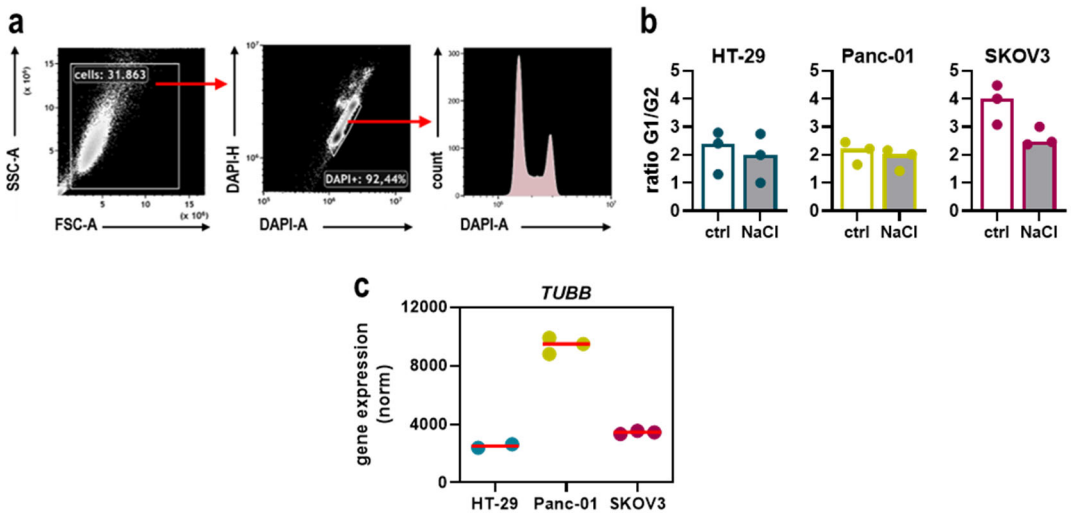

Fig. S9. Cell cycle analysis and *TUBB* expression in NaCl-treated controls compared to incubation with fully supplemented cell culture medium in the first 2 h of experiments. (**a**) representative flow cytometry dot plots and intensity histograms of gating strategy for cell cycle analysis; (**b**) G1/G2 ratio of tumor cells 24 h after exposure to NaCl compared to culture medium controls; (**c**) normalized gene expression of *TUBB* in HT-29, Panc-01, and SKOV3 cells 4 h after exposure to untreated NaCl. Bar graphs show median. NaCl = 0.9 % saline solutions.

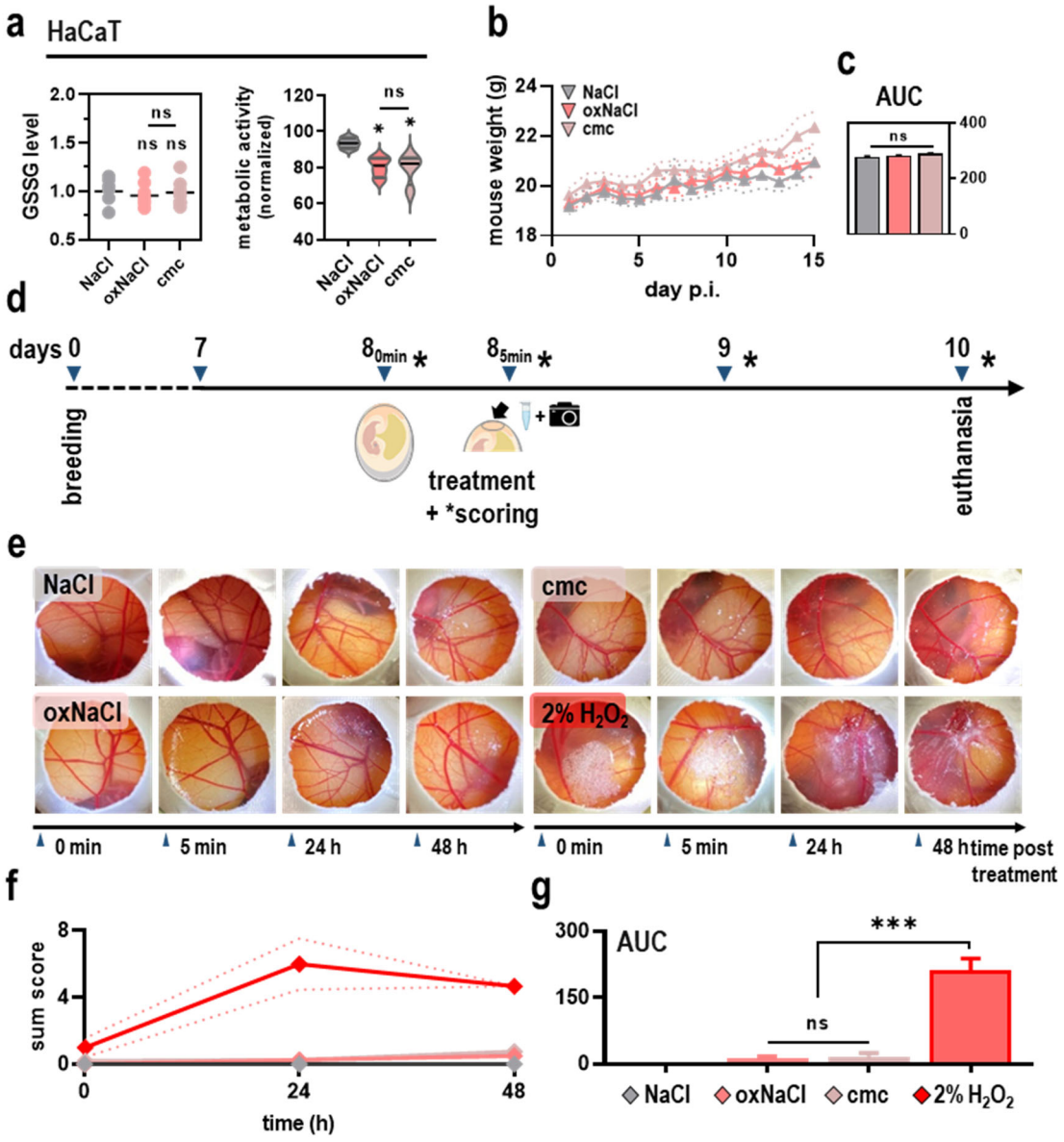

Fig. S10. Safety and irritation potential assessment of oxNaCl and cmc solutions. (**a**) determination of intracellular GSSG levels and metabolic activity of non-malignant HaCaT keratinocytes 24 h after exposure to NaCl, oxNaCl, or cmc; (**b**) mouse weight curves during animal experiments and calculated area under the curve (AUC) thereof (inserted chart); (**c**) scheme of the experimental procedure of the HET-CAM assay; (**d**) representative images of CAM reactions during 48 h after exposure to NaCl, oxNaCl, cmc, or 2 % H_2O_2 (positive control); (**e-f**) assessed sum score (**e**) and calculated area under the curve (AUC) (**f**). Violin plots show median ± interquartile range. Graphs show mean ± SEM. Statistical analysis was performed using one-way analysis of variance (ANOVA) (*p<0.05, ***p<0.001), ns = non-significant. oxNaCl = gas plasma-oxidized saline. cmc = concentration-matched control.

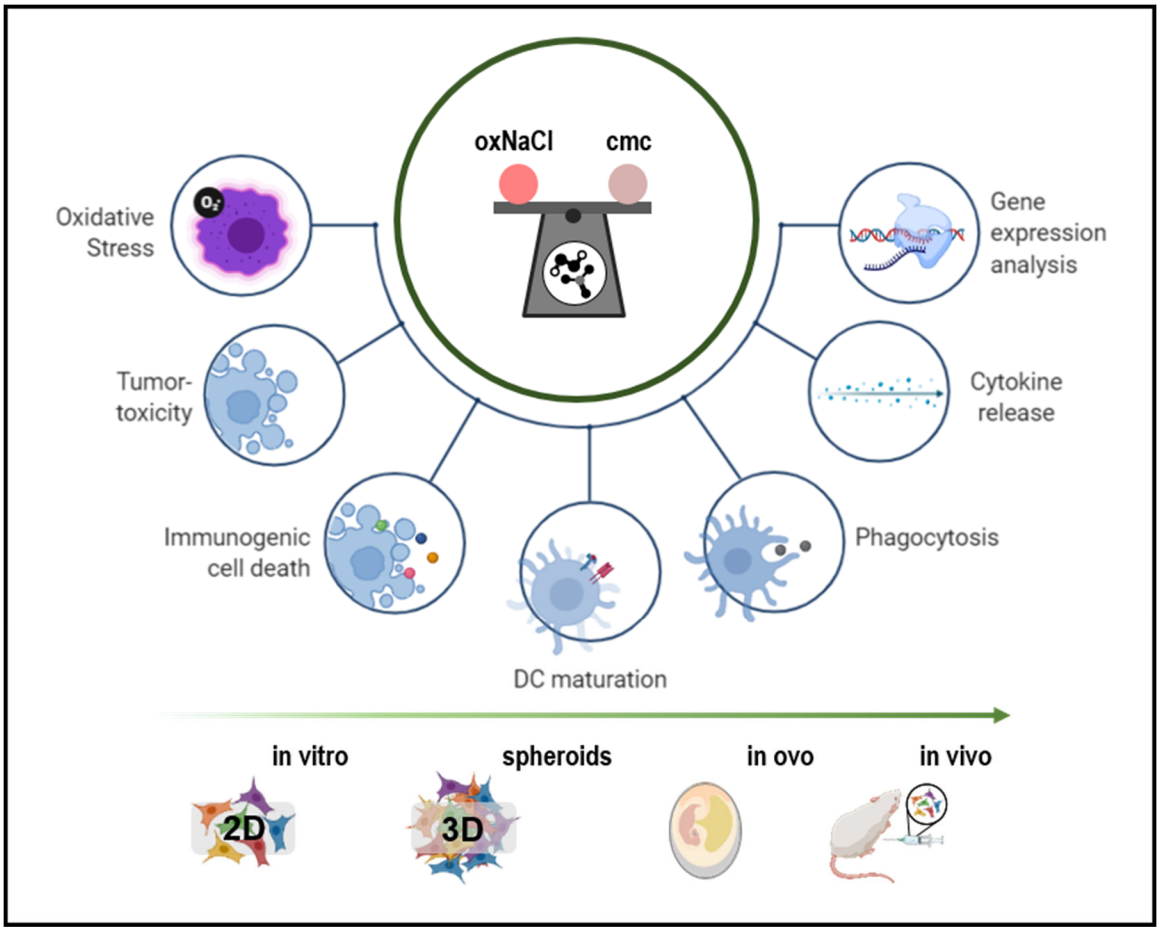

Fig. S11. Study overview of a head-to-head comparison of gas plasma-oxidized sodium chloride (oxNaCl) and an H_2O_2 and NO_3^- concentration-matched control (cmc). Anti-tumor effects of gas plasma-oxidized sodium chloride (oxNaCl) were investigated in a head-to-head comparison with H_2O_2 and NO_3^- concentration-matched control (cmc) liquids in a model of peritoneal carcinomatosis. To that extent, evaluation of intracellular oxidation, tumor toxicity, expression of immunogenic surface markers, tumor cell interaction with dendritic cells, cytokine release, and gene expression profiling was performed. As model systems, 2D cell cultures, 3D tumor spheroids, 3D vascularized tumor organoids grown *in ovo*, and a syngeneic mouse model of peritoneal carcinomatosis were utilized.

Table S1. Characteristics of liquids employed in this study after one freeze-thaw cycle. Shown are the pH and concentrations of hydrogen peroxide (H_2O_2), hypochlorous acid (HOCl), nitrite (NO_2^-), and nitrate (NO_3^-) for untreated sodium chloride (NaCl), gas plasma-oxidized NaCl (oxNaCl), and the concentration-matched control NaCl (cmc).

trait	NaCl	gas plasma-generated oxNaCl	cmc (concentration-matched control)
pH	5.58	5.33	5.48
H_2O_2 (µM)	0	81.7	76.1
HOCl (µM)	0	0	0
NO_2^- (µM)	0	<1	<1
NO_3^- (µM)	0	7.45	8.62

Table S2. Correlation analysis of immunogenic surface marker expression. P-values and Pearson r of correlation analysis of surface marker expression and H_2O_2 and oxNaCl dosage in all (H_2O_2 and oxNaCl), viable (H_2O_2), and dead (H_2O_2) HT-29, and Panc-01 cells.

marker		HT-29				Panc-01			
		H_2O_2			*oxNaCl*	H_2O_2			*oxNaCl*
		alive	*dead*	*all*	*all*	*alive*	*dead*	*all*	*all*
CD47	r	-0.96	-0.95	-0.95	-0.95	-0.84	-0.79	0.99	-0.71
	$log_{10}(p)$	2.00	2.00	2.00	2.00	1.10	0.92	3.00	0.74
CRT	r	0.24	0.96	0.95	0.93	-0.67	0.90	0.99	0.58
	$log_{10}(p)$	0.15	2.10	1.70	1.70	0.66	1.70	3.00	0.51
HMGB1	r	0.85	0.96	0.96	0.98	0.38	0.70	0.75	0.52
	$log_{10}(p)$	1.15	2.00	2.00	2.40	0.28	0.72	0.85	0.43
HSP70	r	0.68	0.96	0.95	0.89	0.15	0.91	0.99	0.63
	$log_{10}(p)$	0.68	2.05	2.00	1.40	0.09	1.52	3.00	0.60
TNFRI	r	0.89	-0.56	0.72	0.04	0.96	0.65	0.99	0.72
	$log_{10}(p)$	1.30	0.49	0.77	0.02	2.10	0.64	2.70	0.77
TNFRII	r	0.76	0.99	0.95	0.90	0.98	1.00	-0.96	0.77
	$log_{10}(p)$	0.85	3.00	2.00	1.40	2.52	3.00	2.05	0.89

References

1. Bekeschus, S.; Schmidt, A.; Weltmann, K.-D.; von Woedtke, T. The plasma jet kinpen – a powerful tool for wound healing. *Clin. Plas. Med.* **2016**, *4*, 19-28, 10.1016/j.cpme.2016.01.001.
2. Clemen, R.; Freund, E.; Mrochen, D.; Miebach, L.; Schmidt, A.; Rauch, B.H.; Lackmann, J.W.; Martens, U.; Wende, K.; Lalk, M.*, et al.* Gas plasma technology augments ovalbumin immunogenicity and ot-ii t cell activation conferring tumor protection in mice. *Adv Sci (Weinh)* **2021**, *8*, 2003395, 10.1002/advs.202003395.
3. O'Brien, J.; Wilson, I.; Orton, T.; Pognan, F. Investigation of the alamar blue (resazurin) fluorescent dye for the assessment of mammalian cell cytotoxicity. *Eur. J. Biochem.* **2000**, *267*, 5421-5426, 10.1046/j.1432-1327.2000.01606.x.
4. Subramanian, A.; Tamayo, P.; Mootha, V.K.; Mukherjee, S.; Ebert, B.L.; Gillette, M.A.; Paulovich, A.; Pomeroy, S.L.; Golub, T.R.; Lander, E.S.*, et al.* Gene set enrichment analysis: A knowledge-based approach for interpreting genome-wide expression profiles. *Proc. Natl. Acad. Sci. U. S. A.* **2005**, *102*, 15545-15550, 10.1073/pnas.0506580102.
5. Mootha, V.K.; Lindgren, C.M.; Eriksson, K.F.; Subramanian, A.; Sihag, S.; Lehar, J.; Puigserver, P.; Carlsson, E.; Ridderstrale, M.; Laurila, E.*, et al.* Pgc-1alpha-responsive genes involved in oxidative phosphorylation are coordinately downregulated in human diabetes. *Nat. Genet.* **2003**, *34*, 267-273, 10.1038/ng1180.
6. Shannon, P.; Markiel, A.; Ozier, O.; Baliga, N.S.; Wang, J.T.; Ramage, D.; Amin, N.; Schwikowski, B.; Ideker, T. Cytoscape: A software environment for integrated models of biomolecular interaction networks. *Genome Res.* **2003**, *13*, 2498-2504, 10.1101/gr.1239303.
7. Liedtke, K.R.; Diedrich, S.; Pati, O.; Freund, E.; Flieger, R.; Heidecke, C.D.; Partecke, L.I.; Bekeschus, S. Cold physical plasma selectively elicits apoptosis in murine pancreatic cancer cells in vitro and in ovo. *Anticancer Res.* **2018**, *38*, 5655-5663, 10.21873/anticanres.12901.
8. Bender, C.; Matthes, R.; Kindel, E.; Kramer, A.; Lademann, J.; Weltmann, K.D.; Eisenbeiss, W.; Hubner, N.O. The irritation potential of nonthermal atmospheric pressure plasma in the het-cam. *Plasma Process. Polym.* **2010**, *7*, 318-326, 10.1002/ppap.200900119.
9. Bekeschus, S.; Wende, K.; Hefny, M.M.; Rodder, K.; Jablonowski, H.; Schmidt, A.; Woedtke, T.V.; Weltmann, K.D.; Benedikt, J. Oxygen atoms are critical in rendering thp-1 leukaemia cells susceptible to cold physical plasma-induced apoptosis. *Sci. Rep.* **2017**, *7*, 2791, 10.1038/s41598-017-03131-y.